Soft Matter

Dynamic Article Links

Cite this: *Soft Matter*, 2012, **8**, 9235

www.rsc.org/softmatter

**PAPER**

# Uptake of hydrogel particles with different stiffness and its influence on HepG2 cell functions†

**Weijun Liu, Xiangyan Zhou, Zhengwei Mao,* Dahai Yu, Bing Wang and Changyou Gao***

***Received 28th April 2012, Accepted 4th July 2012***
**DOI: 10.1039/c2sm26001h**

The interactions between colloidal particles and cells are of paramount importance for understanding the potential safety issue of the particles, which in turn provide the design principles of various carriers for biomedical applications. In this study, the influence of particle stiffness on cellular uptake and cell functions are elucidated. Four types of poly(2-hydroxyethyl methacrylate) (HEMA) hydrogel particles with different amounts of crosslinking agent, *N*,*N*′-methylene-bis-acrylamide (BIS), and thereby compressive modulus (from 15–156 kPa) were synthesized by an emulsion–precipitation polymerization. All of the particles had a diameter of 800–1000 nm in water. Although the softer particles were slightly swollen in the cell culture medium, the particle sizes were still similar. Adsorption of proteins (35 mg $g^{-1}$ particles) occurred on all the particles, leading to a change of zeta potential from −20 mV (in water) to −5 mV (in serum containing medium). However, the particle size and surface charge property were not significantly changed. The softer particles were internalized by HepG2 cells at a faster rate and larger amount than the stiffer particles. Cellular uptake mechanisms were clarified by the addition of inhibitors to specific endocytosis pathways. The influence of the particle uptake on cell toxicity and functions were then studied in terms of cell viability, morphology and cytoskeleton organization, and cell adhesion. Uptake of all types of the particles did not cause an apparent decrease of cell viability and alteration of cell morphology, but changed the cytoskeleton organization to some extent. The cell adhesion ability was significantly affected, especially after uptake of the stiffer particles.

## 1. Introduction

Colloidal particles have a typical size of 1 nm to microns. They can be classified as tiny particles, molecular aggregates (*e.g.* micelles) and even a single molecule (*e.g.* dendrimer and protein).[1,2] Over the past a few decades colloidal particles have had more and more important roles in the biological field along with the fast development of nanotechnology and biotechnology. They can be used as carriers for controlled drug release,[3,4] gene therapy,[5,6] disease diagnosis,[7] and bio-imaging.[8–10]

During the applications of colloidal particles in the biomedical field they will inevitably interact with the cells and tissues, leading to their internalization into living cells. On one hand, uptake of the particles may bring some unexpected side effects, for example, toxicity and more substantial influence on cell functions.[11,12] On the other hand, many of the biological applications of particles are dependent on their cellular uptake, for example, intracellular drug and gene delivery. In these situations, the particles should be transported through cell membrane and be able to travel into the cytosol. Therefore, it is urgent to understand the interaction between colloidal particles and cells. It is of particular importance to clarify the relationship between the chemical and physical properties of particles and responses of cells, including uptake kinetics and pathways, intracellular distribution, and change of cellular functions.

So far it has been found that the size,[13] shape,[14] surface chemistry,[15] and surface charge[16] of colloidal particles have a big impact on the cellular uptake processes and intracellular distribution. Cellular uptake can take place when cells are exposed to various kinds of colloidal particles with a diameter ranging from several nanometers to microns by adsorptive and/or receptor-mediated endocytosis pathways.[17] Generally, the largest uptake amount is achieved when the particles have a diameter around 100 nm. Influence of the particle shape is more complicated than that of the size, and thus is scarcely discussed. Nonetheless, results have demonstrated that cells can ingest colloidal particles with various shapes including spheres, rods,[18,19] tubes,[20] and sheets.[21] Up to the present, the surface properties of the colloidal particles are the most important and widely studied parameter

*MOE Key Laboratory of Macromolecular Synthesis and Functionalization, Department of Polymer Science and Engineering, Zhejiang University, Hangzhou 310027, People's Republic of China. E-mail: zwmao@zju.edu.cn; cygao@mail.hz.zj.cn; Fax: +86-571-87951108; Tel: +86-571-87951108*

† Electronic supplementary information (ESI) available. See DOI: 10.1039/c2sm26001h

for cellular uptake because in most cases they provide essential driving forces for the uptake and decide the uptake pathways. For example, a positively charged surface is feasible for cellular uptake owing to the negatively charged cell surface. Various ligands with specific binding ability to cell membrane, intracellular organelles and even nucleus can be conjugated to the colloidal particles, leading to specific recognition and enhanced uptake by specific cells (*e.g.* cancer cells),[22] and altered intracellular distribution.[23]

Amongst all other properties, mechanical properties are an important factor regulating biological responses, yet are often neglected in cellular uptake studies. For example, erythrocytes are able to avoid filtration in spleen because of their discoidal shape and mechanical flexibility. The mechanical properties of the cellular microenvironment have an important role in the morphogenesis of tissues such as bone, cartilage and cornea.[24,25] Thus, it would be reasonable to suspect that the mechanical properties of particles can dramatically affect cellular uptake. Within the very limited reports on this topic, Beningo and Wang found that macrophages preferably engulf rigid microparticles of identical chemical properties.[26] Banquy *et al.* prepared a series of hydrogel nanoparticles (~150 nm in diameter) with different stiffness and studied their influence on cellular uptake routes and kinetics in RAW 264.7 macrophages. Soft and stiff nanoparticles are preferentially internalized by macropinocytosis and clathrin-mediated routes, while those with intermediate elasticity were found to be internalized *via* multiple mechanisms, resulting in a faster uptake rate.[27]

It is known that particle size can strongly affect the uptake process and mechanism. Colloidal particles can be imported into cells *via* pinocytosis for smaller particles (<0.2 μm) and phagocytosis for larger particles (>0.5 μm).[28] Thus, it would be interesting to understand the influence of relatively big particles (around 1 μm in diameter) with different mechanical properties on the cellular uptake processes and mechanisms as well as their intracellular fate. On the other hand, the mechanical properties of particles might influence the interactions between particles and intracellular organs, and thereby influence the cell viability and functions. Therefore, investigation of the internalization process of colloids with different mechanical properties and their influence on cell functions is of critical importance.

The liver is known to be the main organ where metabolism and detoxification take place. When particles are injected into blood, a large portion would be accumulated in liver. Moreover, many drug delivery systems are targeted to treat liver diseases. Therefore, liver cells will inevitably encounter the intravenously injected NPs, leading to cellular ingestion, and in turn a change in their functions. In this study hepatoblastoma cell line HepG2 cells shall be used because they retain many of the specialized liver functions such as secretion of major plasma proteins, which are normally lost by primary hepatocytes in culture.[29]

In this work, hydrogel particles with variable mechanical strength are synthesized by using different concentrations of cross-linker molecules. Their basic chemical and physical properties such as chemical structure, morphology, size and surface properties are characterized. Cellular uptake kinetics, mechanism and intracellular localization of these particles are studied. Toxicity and changes of cell functions are also studied in terms of cell viability, cell adhesion and cytoskeleton organization. These results will provide insight understanding of the interactions between cells and colloidal particles with different mechanical properties, and highlight the importance of particle stiffness for intravenous applications and intracellular drug delivery.

## 2. Experimental

### 2.1. Materials

2-Hydroxyethyl methacrylate (HEMA, Sigma-Aldrich) was vacuum distilled prior to use. *N*,*N*′-Methylene-bis-acrylamide (BIS, Sigma-Aldrich) was used as the crosslinking agent and was re-crystallized twice from hexane. Potassium persulfate (KPS, Shanghai Chemical Reagents Co., Ltd. China) was re-crystallized from Milli-Q® water. Sodium dodecyl sulfate (SDS) was purchased from Haotian Co., Ltd. China. BCA kit was purchased from KeyGEN Co. Ltd. China. 2,5-Diphenyltetrazolium bromide (MTT), amiloride-HCl, amantadine-HCl, sodium azide, genistein, cytochalasin D (CytD), and 4,6-diamidino-2-phenylindole (DAPI) were purchased from Sigma-Aldrich. The regular growth medium for the cells is high-glucose DMEM (Gibco, USA) supplemented with 10% fetal bovine serum (FBS), 100 U $mL^{-1}$ penicillin, and 100 μg $mL^{-1}$ streptomycin. The water was purified *via* a Milli-Q® Gradient System equipped with a quantum™ cartridge, and had a resistivity of 18.2 MΩ cm. Other chemicals were of analytical grade and used as received.

### 2.2. Synthesis of hydrogel particles with different mechanical properties

The monomer HEMA and crosslinker BIS with various ratios (listed in Table 1, the total amount was 4 g) were added into 145 mL of water containing 0.04 g of SDS and stirred for 30 min with a magnetic stirrer. After purged with nitrogen the mixture solution was heated to 75 °C under continuous mechanical agitation (200 rpm per min). An aqueous solution of KPS (0.12 g in 5 mL water) was subsequently added to the medium. The polymerization was maintained for 12 h under a nitrogen atmosphere to ensure maximum conversion and then was cooled to room temperature. The acquired hydrogel particles were purified by dialysis for 1 week against water to remove the surfactants and other small molecules. They were further labeled with rhodamine B (RdB) using a standard coupling reaction of *N*,*N*-dicyclohexylcarbodiimide/4-dimethylaminopyridine (DCC/DMAP), as described previously.[30] The labeled hydrogel particles were purified by dialysis in a water–ethanol (1 : 1) mixture for 2 weeks. The rhodamine B-labeled hydrogel particles were used throughout this work.

The concentration of obtained hydrogel particles was determined by testing the solid weight of 1 mL of the particles suspension after freeze-drying. Four different batches of hydrogel particles were prepared using four different BIS concentrations (3%, 5%, 10% and 15%), respectively. The particles were denoted as HEMA-BIS3%, HEMA-BIS5%, HEMA-BIS10%, and HEMA-BIS15%, respectively. A detailed recipe of the reaction is summarized in Table 1.

 

**Table 1** Theoretical recipe and found compositions of HEMA-BIS hydrogel particles

| Sample | HEMA (g) | BIS (g) | Theoretical BIS content (%) | Theoretical N content (%) | Found N content (%) | Found BIS content (%) |
|---|---|---|---|---|---|---|
| HEMA-BIS3% | 3.88 | 0.12 | 3 | 0.55 | 0.463 | 2.53 |
| HEMA-BIS5% | 3.80 | 0.20 | 5 | 0.78 | 0.696 | 4.31 |
| HEMA-BIS10% | 3.60 | 0.40 | 10 | 1.64 | 1.43 | 8.72 |
| HEMA-BIS15% | 3.40 | 0.60 | 15 | 2.36 | 1.98 | 12.59 |

### 2.3. Characterizations of hydrogel particles

**2.3.1. Chemical composition of hydrogels particles.** The hydrogel particles were freeze-dried and characterized by Fourier transform infrared (FTIR) spectroscopy (Vector 22 spectrometer, Bruker). The percentage of nitrogen, hydrogen and carbon elements in the hydrogel particles was analyzed by elemental analysis (Flash EA 1112, Thermo Finnigan) to calculate the relative content of BIS.

**2.3.2. The mechanical properties of bulk hydrogels.** The macroscopic hydrogels (cylindrical shape, 12 mm in diameter and 10 mm in height) which have the identical chemical compositions as their corresponding particles were prepared by bulk polymerization in a mold. Their mechanical properties were measured and were used to estimate the micromechanical properties of the corresponding particles. The bulk hydrogels were compressed by a mechanical tester (Instron 5543, USA) in a water tank containing phosphate buffered saline (PBS) at 37 °C at a rate of 10% per min until failure occurred. The compressive modulus of the bulk hydrogels was obtained from the linear region in the 3–5% strain. Each value was averaged from 4 parallel experiments.

**2.3.3. Morphology, size, surface charge and protein adsorption of hydrogel particles.** A drop of hydrogel particles suspension was applied onto a clean glass slide. After being dried in air, the morphology of the hydrogel particles was observed under field-emission scanning electron microscopy (FESEM, JEOL JSM-6700) at an accelerating voltage of 10 kV.

The size and surface charge of the hydrogel particles were determined using Beckman Delsa™ Nano (Beckman Coulter). To study the colloidal stability in cell culture medium, the hydrogel particles were incubated in PBS and DMEM/10% fetal bovine serum (FBS) medium for different time.

After the hydrogel particles were incubated in DMEM/10% FBS for different time, the adsorbed proteins on the particles were rinsed off by 5% SDS solution under ultrasonication for 1 h. The supernatant was collected by centrifugation at 15 000 rpm for 15 min and was used to determine protein concentration by a BCA kit following the manufacturer's instruction.

### 2.4. Cellular uptake and intracellular distribution

**2.4.1. Cell culture.** The human HepG2 cells were obtained from the American Type Culture Collection (ATCC) and maintained with a regular growth medium consisting of high-glucose DMEM (Gibco, USA) supplemented with 10% fetal bovine serum, 100 U $mL^{-1}$ penicillin, 100 μg $mL^{-1}$ streptomycin, and cultured at 37 °C in a 5% $CO_2$ humidified environment.

**2.4.2. Cellular uptake of hydrogel particles with different modulus.** The cells were seeded on a 24-well plate at a density of $1 \times 10^5$ cells per well and allowed to attach overnight. To determine the particle uptake rate and amount as a function of particle concentration and incubation time, the cells were incubated with various concentrations of RdB-labeled hydrogel particles for 24 h or incubated with 50 μg $mL^{-1}$ hydrogel particles for different time, respectively. The cells were then washed 3 times with PBS to remove the free particles and detached by trypsin. Finally, the uptake amount of the particles was determined by flow cytometry (FACS Calibur, BD).

To determine the uptake mechanism of the particles, the energy dependence of cell–particle interaction was assessed by treatment with sodium azide. Different pharmacological inhibitors, including 2 mM amiloride-HCl, 1 mM amantadine-HCl, 100 mM genistein, and 10 μg $mL^{-1}$ cytochalasin D were used to treat the HepG2 cells for 1 h before incubation with the four types of hydrogel particles, respectively.

**2.4.3. Intracellular distribution.** Fluorescent staining of lysosomes and cell nuclei was performed to display the intracellular distribution of hydrogel particles by confocal laser scanning microscopy (CLSM, LSM 510, Carl Zeiss). Briefly, after being cultured with 50 μg $mL^{-1}$ hydrogel particles for the desired time, the cells were carefully washed 3 times with PBS, and continually cultured with LysoTracker® Green and DAPI at 37 °C for another 30 min, respectively.

**2.4.4. Cell mortality and cell viability.** The HepG2 cells were plated at a density of $2 \times 10^4$ cells per well in a 96-well plate and cultured overnight. The medium was replaced with the medium containing different hydrogel particles of varying concentrations. To determine the cell mortality, after being co-incubated with particles for 24 h the medium was removed and the cells were washed 3 times with PBS. 50 μg $mL^{-1}$ PI solution was added and the cells were incubated for another 30 min in the dark. The cellular average fluorescence intensity was measured by flow cytometry and analyzed by the CellQuest Pro software. To determine the cell viability, after being co-incubated with 50 μg $mL^{-1}$ hydrogel particles of different modulus for 24 h, 20 μL MTT (5 mg $mL^{-1}$) was added to each well and the cells were further cultured at 37 °C for 4 h. The dark blue formazan crystals generated by mitochondrial dehydrogenase in living cells were dissolved by dimethyl sulfoxide (DMSO). The absorbance at 570 nm was measured by a microplate reader (Biorad Model 550).

**2.4.5. Cell adhesion assay.** The cells were seeded on a 6-well plate at a density of $3 \times 10^5$ cells per well and cultured overnight. After being treated with 50 μg $mL^{-1}$ hydrogel particles for 24 h,

the cells were washed with PBS 3 times and detached with trypsin. They were counted under a hemacytometer and then plated into a 24-well plate with an equal number per well and allowed to adhere for 3 h and 24 h, respectively. Untreated cells were used as control. After the non adherent cells were washed away with PBS, the adherent cells were counted at 10 different areas under an optical microscope. The quantification was repeated twice and each sample was assayed in triplicate. The average value of each sample was normalized to the particle-free control.

**2.4.6. Scanning electron microscopy for cell morphology.** To observe the cell morphology under SEM, the cells were washed with PBS and fixed with 2.5% glutaraldehyde in PBS at 4 °C for 48 h after being co-cultured with the hydrogel particles for 24 h. After they were washed with PBS to remove the remnant glutaraldehyde, the cells were dehydrated with a graded series of ethanol. The cells were further dehydrated with acetone and treated with isoamyl acetate. After they were dried by a critical point drying method, the cells were sputtered with a thin layer of platinum and observed under SEM (FESEM, JEOL JSM-6700) at an accelerating voltage of 10 kV.

**2.4.7. Cytoskeleton observation by CLSM.** The cells were seeded on a 35 mm Petri dish at a density of $3 \times 10^5$ cells per well and cultured overnight. After they were treated with the hydrogel particles at a concentration of 50 μg $mL^{-1}$ at 37 °C for 24 h, the cells were washed with PBS 3 times, fixed with 4% paraformaldehyde in PBS for 30 min, and then permeabilized with 0.5% Triton X-100 at 4 °C for 5 min. They were then incubated in 1% bovine serum albumin (BSA)/PBS at 37 °C for 30 min to block non-specific bindings. The cells were subsequently treated with 0.15 μM rhodamine-conjugated phalloidin (Molecular Probes, USA) for 20 min and the nuclei were stained by incubation with 2 μg $mL^{-1}$ DAPI (Sigma, USA) for 10 min in dark. The cytoskeletons were then observed by CLSM.

**2.4.8. Statistical analysis.** All values were expressed as mean ± standard deviation (SD). Statistically significant value is set as $p < 0.05$ based on one-way analysis of variance (ANOVA) in the Origin software using the Tukey Means Comparison method.

## 3. Results and discussion

### 3.1. Characterization of hydrogel particles

All the hydrogel particles were synthesized by mini-precipitation polymerization at a constant monomer + crosslinker amount of 4 g with 4 different ratios of BIS (From 3% to 15%, Table 1). The chemical structure of the hydrogel particles was characterized by FTIR (Fig. 1). The peaks at $1724^{-1}$ $cm^{-1}$ and 1164 $cm^{-1}$ are assigned to characteristic absorption bands of ester carbonyl groups C=O and C–O of pHEMA, respectively. Compared to the pure pHEMA polymer, a peak at 1540 $cm^{-1}$ appeared. This is a typical characteristic absorption band of C=O in acylamino bond of the BIS unit, whose relative intensity increased along with the BIS feeding amount. The absorption at 3425 $cm^{-1}$ is the overlapping peak of β-OH in pHEMA and N–H bond in acylamino of BIS unit. Elemental analysis found that the N%

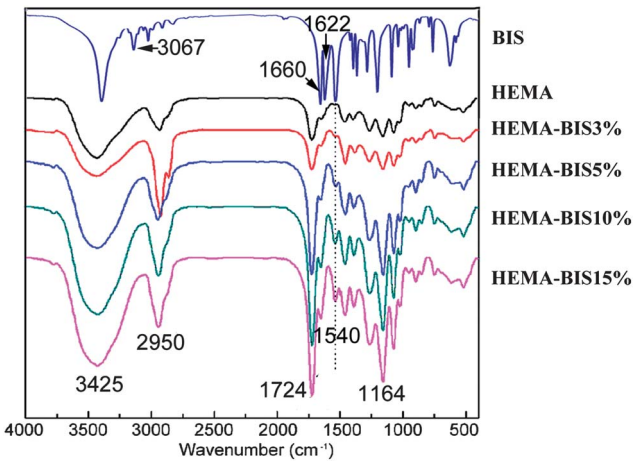


**Fig. 1** FTIR spectra of HEMA, BIS and different hydrogel particles.

increased with the increase of BIS feeding amount (Table 1). The found BIS contents in the hydrogel particles are consistent with their feeding ratios, confirming the successful manipulation of crosslinking degree of the hydrogel particles.

The compressive modulus of the bulk hydrogels was detected by a compressing method and presented in Fig. 2. With the increased BIS content, the modulus was gradually enhanced from 16.7 kPa (HEMA-BIS3%) to 155.7 kPa (HEMA-BIS15%), a variation of 1 order of magnitude. Since all the hydrogel particles have exactly the same chemical compositions and are synthesized at the same conditions as those of the respective bulk hydrogels, it is reasonably to assume that they possess the same modulus or at least are in the same range.

All of the hydrogel particles were well dispersed and had a diameter around 800–1000 nm in water. When dispersed in cell culture medium containing serum (DMEM/10% FBS, Table 2 and Fig. S1a†) for 24 h, the sizes of the particles with a lower modulus (HEMA-BIS3% and HEMA-BIS5%) increased to

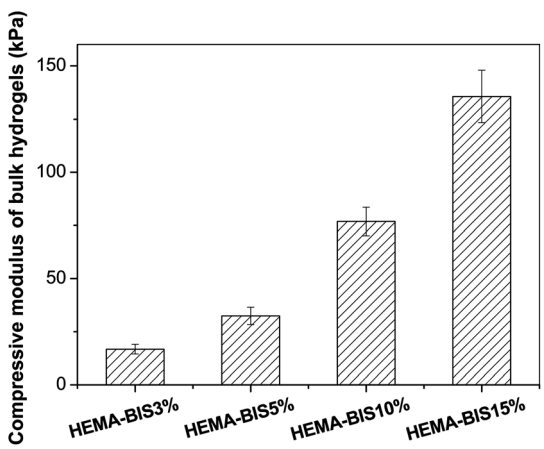


**Fig. 2** Compressive modulus of bulk hydrogels prepared at the same compositions and conditions with the hydrogel particles, respectively. Since both the respective bulk hydrogels and hydrogel particles are prepared at the exactly same conditions, the modulus measured at the linear region of 3–5% strain is regarded as same with that of the hydrogel particles of the same compositions.

**Table 2** Size, protein adsorption and surface zeta potentials of different hydrogel particles in DMEM/10% FBS for 24 h

| | Diameter (nm) | Protein adsorption (mg $g^{-1}$) | Zeta potential (mV) |
|---|---|---|---|
| HEMA-BIS3% | 1264.7 ± 122.8 | 42.3 ± 5.6 | −4.3 ± 0.8 |
| HEMA-BIS5% | 1214.7 ± 102.8 | 41.3 ± 6.3 | −5.5 ± 1.2 |
| HEMA-BIS10% | 1059.4 ± 101.4 | 42.8 ± 6.1 | −5.3 ± 1.0 |
| HEMA-BIS15% | 960.6 ± 96.6 | 43.5 ± 2.3 | −5.4 ± 0.8 |

about 1200 nm, whereas those with a higher modulus did not change obviously. This might be attributed to the swelling of the weakly cross-linked hydrogel particles and/or the slight aggregation of the softer particles in the salts-containing buffers which can shield electrostatic repulsion.

All of the hydrogel particles were negatively charged (−20 mV) in water, which might be attributed to the –OH groups from pHEMA molecules. When these particles are used for the study of cell–particle interactions in culture medium, their surface properties will be more important than the bulk chemical compositions.[31] Indeed, the particle surfaces are inevitably decorated with many biomolecules, especially a selected group of proteins from the culture medium. Therefore, the cell will interact with the decorated surface rather than the pristine one. As shown in Table 2 and Fig. S1b,† protein adsorption on the hydrogel particles occurred prominently after 1 h incubation (~35 mg per gram particles). The adsorbed protein amount was slightly increased and reached the highest value of ~40 mg per gram particles at 24 h. However, protein exchange cannot be excluded due to the so-called Vroman effect.[32] Nevertheless, each of the 4 types of particles showed similar protein adsorption ability during the whole experiment period.

In addition to adsorbed proteins, the surface charge density of the particles is another important parameter for a therapeutic delivery system, due to its close association with the cellular uptake.[33,34] Due to the electrostatic screening and/or protein adsorption in the culture medium, the surface charge will be significantly influenced by environmental conditions, as confirmed in Table 2 and Fig. S1c and d.† The zeta-potential of the hydrogel particles was slightly changed from −20 mV to −10 mV upon incubation in PBS. It further changed to −5 mV due to the adsorption of zwitterionic proteins in DMEM/10% FBS, and remained unchanged for the remaining experimental period (24 h). Again, the 4 types of particles showed a similar surface charge property. Therefore, the size and surface properties of the 4 types of particles are roughly same in the cell culture environment (Table 2), and are not considered as the governing factors for the cellular uptake of the hydrogel particles of different mechanical strength. Therefore, in this case it is possible to correlate the mechanical property of the hydrogel particles with the cellular uptake and cell functions.

The morphology of these hydrogel particles was observed under FESEM (Fig. 3). The HEMA-BIS3% particles were completely collapsed, while the HEMA-BIS10% and HEMA-BIS15% particles showed very little deformation after drying. This difference reflects the different stiffness of the particles as well, which is in good agreement with their chemical structures and mechanical strength (Fig. 2). The size of the particles in a dry state was measured to be 400–600 nm *via* software Image J, which is smaller than that in the wet state (Table 2 and Fig. S1a†). This inconsistency is a universal phenomenon for hydrogel particles, and is caused by particle shrinkage after drying. Moreover, the shrinkage extent was different for the softer and the stiffer particles.

### 3.2. Cellular uptake

Since the hydrogel particles are covalently labeled with a fluorescent dye, rhodamine B, they can be detected by both fluorescence microscopy and flow cytometry. Normalization of the fluorescence intensity of each type of the rhodamine B-labeled particles (by fluorescence spectroscopy at the same concentration) was performed for quantitative measurement by FCM. In the FCM measurement, the logarithmic fluorescence intensity of untreated cells was set between $10^0$ and $10^1$, and those cells with an intensity higher than $10^1$ were considered to be positive (the cells that had internalized fluorescent hydrogel particles).[35]

As shown in Fig. 4a, at a fixed incubation time of 24 h, the hydrogel particles that internalized into or adsorbed onto the cells increased almost linearly along with the increase of particle concentration, regardless of their stiffness. However, the stiffness does influence the uptake rate and amount. The particles can be categorized into two groups: the softer particles (HEMA-BIS3% and HEMA-BIS5%) and the stiffer particles (HEMA-BIS10% and HEMA-BIS15%). At each fixed particle concentration, the softer hydrogel particles were more significantly internalized with a faster rate than the stiffer particles ($p < 0.05$). The higher uptake of the softer particles was also found at a fixed particle concentration of 50 μg $mL^{-1}$ (Fig. 4b), leading to about 1.5 times

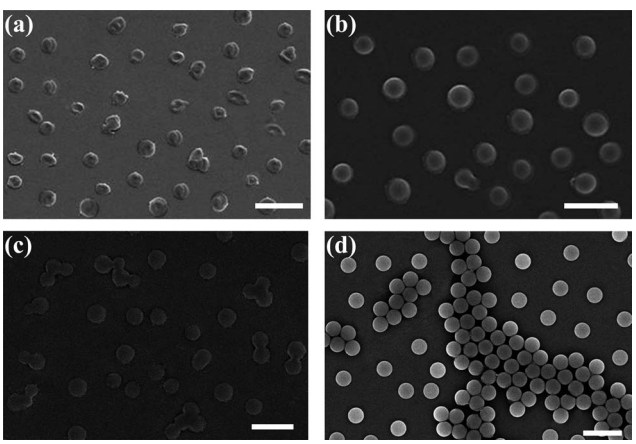


**Fig. 3** SEM images of (a) HEMA-BIS3%, (b) HEMA-BIS5%, (c) HEMA-BIS10%, and (d) HEMA-BIS15% hydrogel particles. Scale bar 1 μm.

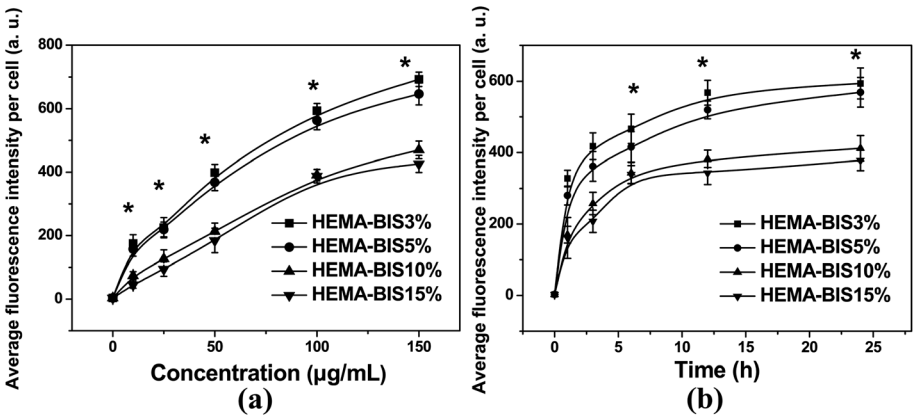


**Fig. 4** Uptake of hydrogel particles by HepG2 cells as a function of (a) particle concentration with a culture time of 24 h, and (b) culture time with a particle concentration of 50 μg $mL^{-1}$. Asterisk indicates significant difference at $p < 0.05$ level.

more than the stiffer particles at 24 h. Fig. 4b shows also that the uptake was very fast during the first several hours, and then gradually leveled off after 6 h. In all the cases, no significant difference was found between the two softer particles and the two stiffer particles ($p > 0.05$). These results disclose that the HepG2 cells preferably internalize the softer particles over the stiffer particles. As reported by Banquy *et al.*, macrophage cells preferably ingest hydrogel nanoparticles (~160 nm in diameter) of medium stiffness (35–130 kPa) with a faster rate and larger amount than soft or stiff nanoparticles.[27] The discrepancy between the results could be attributed to the different cell models as well as the different particle size. It is known that different cells have different capability and specific pathways to engulf exogenous particles owing to their adaption for specific functions. Moreover, the size of the hydrogel particles may also influence the uptake pathway,[28] resulting in different uptake rate and amount. Furthermore, the influence of different testing methods for the mechanical properties cannot be excluded.

It is known that extracellular substances are transported into cells through several different pathways such as transmembrane diffusion, pinocytosis, and receptor-mediated or nonspecific endocytosis.[36,37] To determine the uptake mechanism of the particles with different stiffness, special inhibitors were used to treat the cells before co-incubation with the particles. The uptake ratios of the hydrogel particles by the inhibitors-treated cells were normalized to those of the non-treated cells and presented in Fig. 5. Sodium azide was used as a metabolic inhibitor since it prevents the production of ATP by interfering with the glycolytic and oxidative metabolic pathways of cells. After treatment the internalized amounts of the softer particles (HEMA-BIS3% and HEMA-BIS5%) and stiffer particles (HEMA-BIS10% and HEMA-BIS15%) were significantly decreased to ~50% and ~40% of those of the non-treated control cells ($p < 0.05$), respectively, suggesting that the uptake process is energy-dependent.

There are several possible endocytic pathways for internalization of exogenous particles, including clathrin-mediated endocytosis, caveolae-mediated endocytosis, macropinocytosis and clathrin–caveolae-independent endocytosis.[38] Thus, the specific endocytic pathways were determined by addition of amiloride-HCl, amantadine-HCl, and genistein into the culture medium. Amiloride is an inhibitor of the $Na^+/H^+$ exchange protein and was used to hinder macropinocytosis, which is known as a pathway for uptake of bigger particles (>500 nm).[39] After amiloride treatment the cellular uptake of all types of the particles was significantly decreased to 30–40% of those of the non-treated control cells ($p < 0.05$), indicating that the uptake is mediated by macropinocytosis. CytD can destroy cytoskeleton, and thereby has a strong impact on particle transportation in cells. When the cells were treated with CytD, the uptake amounts of all the samples were significantly decreased to ~50% of those of the non-treated control cells ($p < 0.05$), indicating that cytoskeleton organization is mandatory for the particle uptake. Amantadine was used for the specific inhibition of clathrin-mediated endocytosis as it is known to impede the formation and budding of clathrin-coated pits.[40] When the cells were treated with amantadine-HCl, the internalization ability of the cells

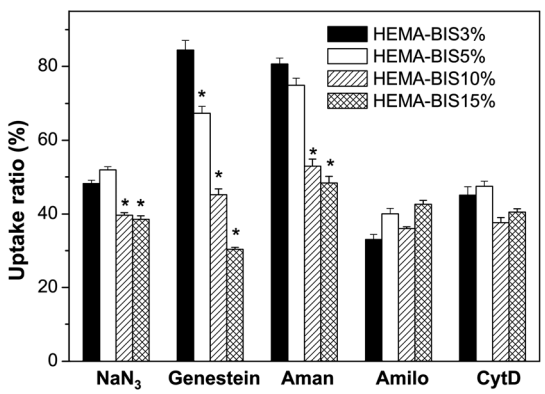


**Fig. 5** Influence of pharmacological inhibitors on uptake of hydrogel particles with different modulus. The cells were cultured without or with pretreatment by amantadine-HCl (Aman, 1 mM, inhibitor of clathrin-mediated endocytosis), genistein (Ge, 100 mM, inhibitor of caveolae-mediated endocytosis), amiloride-HCl (Amilo, 2 mM, inhibitor of macropinocytosis), $NaN_3$ (inhibit energy-dependent process) or cytochalasin D (CytD, 10 μg $mL^{-1}$, inhibitor of cytoskeleton) for 1 h. All the samples have significant difference ($p < 0.05$) *vs.* their respective inhibitor-free controls. Asterisk indicates significant difference at $p < 0.05$ between particles of different stiffness, where the BIS3% particles are used as a reference.

 

decreased significantly to ~80% (HEMA-BIS3%) and 50% (HEMA-BIS15%) ($p < 0.05$) compared with those of the non-treated control cells. It is well known that genistein perturbs cholesterol-rich membrane microdomains which are precursors of caveolae invaginations.[41] Upon treatment, uptake of the particles decreased along with the increase of stiffness, *e.g.* from 84%, 67%, 45% to 30% compared to those of the non-treated control cells. These comparisons suggest that internalization of the stiffer particles is more dependent on both the clathrin-mediated and caveolae-mediated endocytosis. Taking all the results into consideration, one can conclude that there is substantial difference in the uptake mechanisms of the particles with different modulus: the softer particles are mainly internalized *via* macropinocytosis, whereas the stiffer particles are largely endocytosized *via* caveolae- and clathrin-mediated endocytosis as well as macropinocytosis pathways. Our results are basically consistent with those reported by Banquy *et al.*, who found that softer hydrogel particles (~18 kPa) are preferentially internalized by macropinocytosis while uptake of stiffer particles involves the clathrin-mediated route by macrophage cells.[27] Moreover, the different pathways involved in uptake of stiffer particles may be responsible for the different results in two studies too.

### 3.3. Intracellular distribution

To track the intracellular distribution of the hydrogel particles, the lysosomes and cell nuclei were labeled by fluorescent dyes, respectively (Fig. 6). The merged pictures with fluorescent and bright field images confirmed further the cellular colocalization of the particles (column 3). Fig. 6a and e show that only a few particles were colocalized with the lysosomes (yellow color) after 1 h incubation. After 3 h and 12 h incubation, more hydrogel particles overlapped with the lysosomes. A few particles were found in the cytoplasm (red color), implying that part of the hydrogel particles had escaped from the lysosomes. After 24 h incubation, many hydrogel particles were still trapped inside the lysosomes, suggesting the difficulty of lysosome-escape of the present hydrogel particles.

As shown in Fig. 7, the particles were found on the peripheral area of the cells after 1 h incubation and then increased with prolongation of the incubation time. Although many particles were found around the cell nuclei, no colocalization signals of the particles and cell nuclei could be recorded after 24 h co-incubation, suggesting that the particles cannot penetrate into the cell nucleus during the experimental period (Fig. 7d and h). There is no obvious difference in the intracellular distribution of softer and stiffer particles.

### 3.4. Influence on cell functions

Understanding the cytotoxicity and substantial influence on cell functions as a consequence of uptake of colloidal particles is of paramount importance for their applications in biological and medical fields. A cytotoxicity assay is generally adopted,

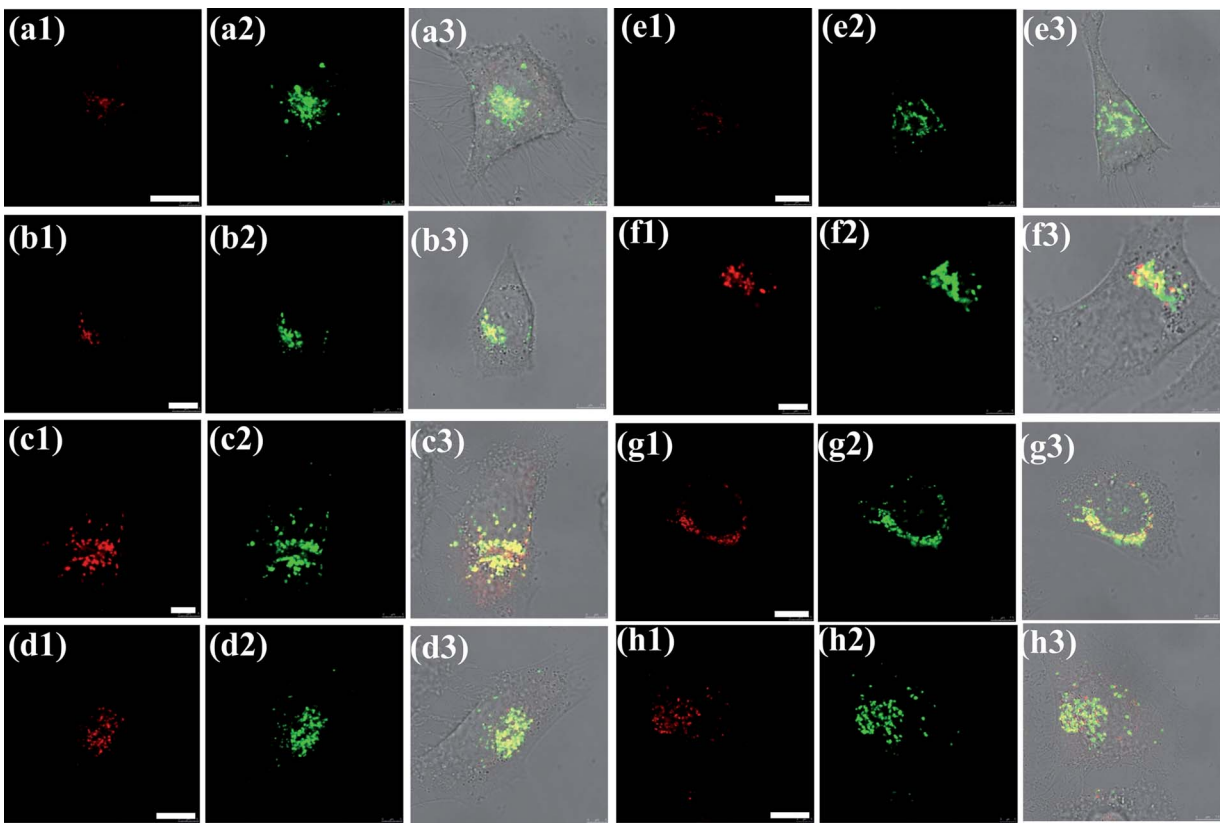


**Fig. 6** CLSM images of HepG2 cells incubated with 50 μg $mL^{-1}$ HEMA-BIS3% (a–d) and HEMA-BIS15% (e–h) particles for different time intervals, respectively. (a and e) 1 h, (b and f) 3 h, (c and g) 12 h, and (d and h) 24 h. The particles and cell lysosomes were stained with red (column 1) and green (column 2), respectively. Column 3 shows merged images of two fluorescent channels and bright field. Scale bar 15 μm.

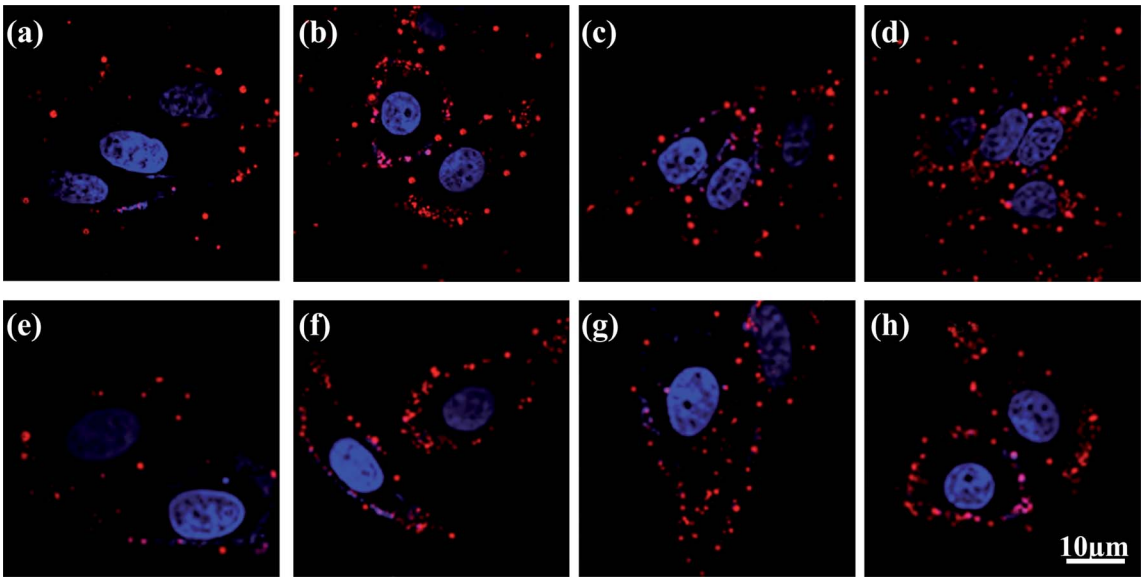


**Fig. 7** CLSM images of HepG2 cells incubated with 50 μg $mL^{-1}$ HEMA-BIS3% (a–d) and HEMA-BIS15% (e–h) particles for different time intervals, respectively. (a and e) 1 h, (b and f) 3 h, (c and g) 12 h, and (d and h) 24 h. The particles and cell nuclei were stained with red and blue, respectively. Scale bar 10 μm.

however, the evaluation of cell functions is more important but is less frequently reported.[42–44] The colloidal particles may become reactive in the cellular environment because of their large surface area per unit mass. It has been confirmed that cellular uptake of colloidal particles can induce a series of cellular responses, leading to the alteration of cell behavior such as proliferation, adhesion, migration, and differentiation. Previously, attention has been paid to the chemical compositions and surface properties of the particles, whereas the influences of mechanical properties of particles on cytotoxicity and cell functions as a consequence of cellular uptake have not been addressed so far. Mechanical properties are known to be an important factor regulating biological responses. For example, the stiffness of a substrate can dominate adhesion and migration of cancer cells as well as differentiation of stem cells.[45,46]

Firstly, after treatment with the hydrogel particles of various concentrations the ratios of dead cells were assessed by PI staining. Fig. 8a shows that less than 10% of the cells were positively stained after 24 h incubation regardless of the particle concentration (up to 150 μg $mL^{-1}$) ($p > 0.05$). No significant difference was found between the softer and the stiffer particles ($p > 0.05$). An MTT assay was further used to assess the viability of the HepG2 cells after they were incubated with 50 μg $mL^{-1}$ particles. Fig. 8b shows that in general the cell viability was largely maintained ($p > 0.05$) regardless of the particle stiffness. Therefore, the hydrogel particles have very weak cytotoxicity regardless of their stiffness and concentration.

However, the cell morphology and its internal skeleton may be disturbed as a result of formation of vacuoles in the cell body during ingestion process, which in turn bring changes to the cellular functions. The cell morphology and actin fibers, which are the main part of the cytoskeleton, were thus observed under FESEM and CLSM, respectively (Fig. 9). The cells co-cultured with the particles show a typical spreading morphology without substantial difference to that of the particle-free cells. Furthermore, the collapsed and spherical particles can be found on the

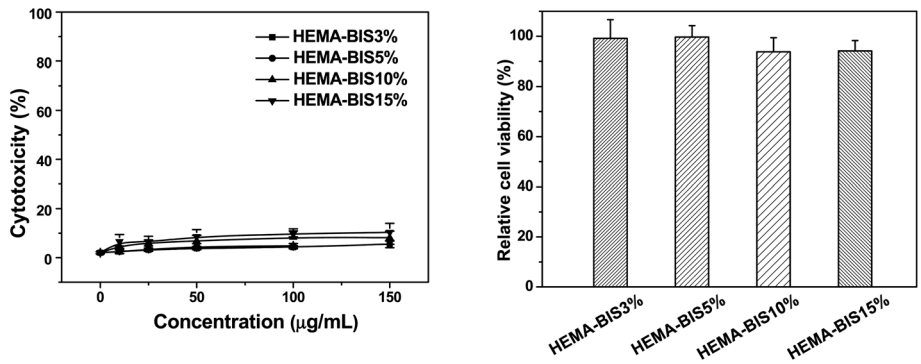


**Fig. 8** (a) Percentage of dead cells detected by PI staining as a function of particle concentration with a culture time of 24 h. (b) Relative viability of HepG2 cells measured by MTT assay after exposure to different hydrogel nanoparticles for 24 h. The data were normalized to that of the particle-free control.

 

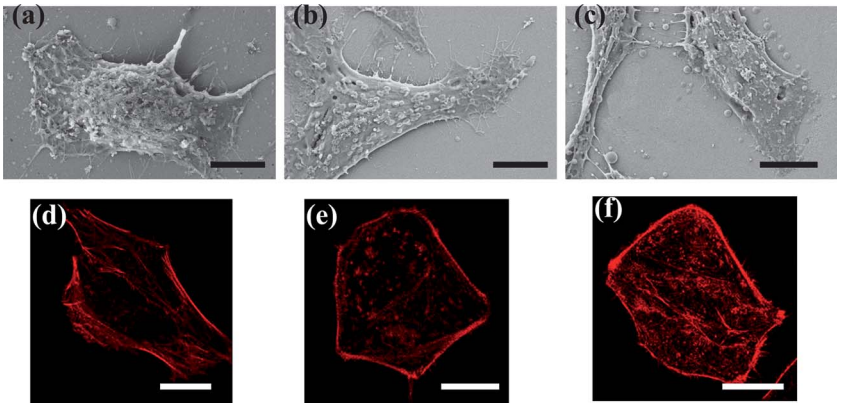


**Fig. 9** (a–c) SEM and (d–f) CLSM images of HepG2 cells before (a and d) and after being cultured with 50 μg $mL^{-1}$ (b and e) HEMA-BIS3% and (c and f) HEMA-BIS15% particles for 24 h, respectively. The F-actin was stained by rhodamine-conjugated phalloidin. Scale bar 5 μm.

cell surface. However, after internalization of the particles the actin organization had changed slightly as viewed under CLSM (Fig. 9d–f). This led to a reduction of the oriented stress fibers regardless of the stiffness of the particles.

The changes in the actin fibers may result in further changes to the cells, especially their adhesion ability. Cell adhesion is the first step for a series of successive cell events, and thereby can govern cell growth, migration, differentiation, survival, and tissue organization. To study the effect of hydrogel uptake on cell adhesion, the cells were exposed to 50 μg $mL^{-1}$ particles for 24 h, detached, and then allowed to adhere for another 24 h. Fig. 10 shows that the relative adhesion percentages of the particles-treated cells were significantly decreased to 83%, 75%, 54% and 58% ($p < 0.05$) for the HEMA-BIS3%, HEMA-BIS5%, HEMA-BIS10%, and HEMA-BIS15%, respectively. The results suggest that uptake of the stiffer particles results in stronger impedance on the cell adhesion ability. Since the softer particles are internalized in larger amounts, the alternation of the cell functions is not chiefly determined by the uptake amount. It is likely that the shape of the stiffer particles is hardly transformed (Fig. 3) within the cells, and may thereby strongly interfere with the adjustment of cell structures during adhesion.

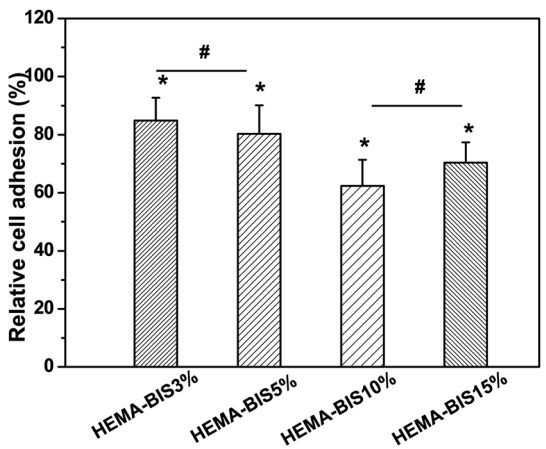


**Fig. 10** Cell adhesion percentage after the cells were pre-cultured with 50 μg $mL^{-1}$ hydrogel particles of different crosslinking degrees, respectively. The data were normalized to those of the particle-free controls. Asterisk indicates significant difference at $p < 0.05$ level, and # indicates insignificant difference at $p < 0.05$ level.

## 4. Conclusions

Four types of pHEMA hydrogel particles with a similar chemical composition, size and surface property but with different mechanical stiffness were synthesized by using different amounts of BIS crosslinking molecules. The softer particles were internalized into HepG2 cells at a faster rate and larger amount than the stiffer particles. All the hydrogel particles were internalized by an energy-dependent mechanism. However, uptake of the particles with different modulus follows different mechanisms: the softer particles are mainly internalized *via* macropinocytosis, whereas the stiffer particles are largely endocytosized *via* caveolae- and clathrin-mediated endocytosis as well as macropinocytosis pathways. The particles were found inside lysosomes with a few released into cytoplasm. However, no particles were found in the cell nucleus after culture for 24 h *in vitro*.

Uptake of all types of the particles apparently did not cause a decrease in the cell viability, but had an influence on the cytoskeleton organization to some extent. The cell adhesion ability was significantly affected, especially after uptake of the stiffer particles. The present study discloses that the stiffness of hydrogel NPs influences their cellular uptake amount, rate, and entry routes. Our results suggest that the mechanical properties of particles are an important factor that control cellular response, and should be carefully considered in designing versatile delivery vehicles and other carriers for biomedical applications.

## Acknowledgements

This work is financially supported by the Natural Science Foundation of China (51120135001, 51003094), the National Basic Research Program of China (2011CB606203), the Zhejiang Provincial Natural Science Foundation of China (Z4090177), the Ph.D. Programs Foundation of Ministry of Education of China (20110101130005), and the Open Project of State Key Laboratory of Supramolecular Structure and Materials (sklssm201224).

## References


1 P. Christian, F. Von der Kammer, M. Baalousha and T. Hofmann, Nanoparticles: structure, properties, preparation and behaviour in environmental media, *Ecotoxicology*, 2008, **17**(5), 326–343, DOI: 10.1007/s10646-008-0213-1.

2 T. Wang and J. L. Keddie, Design and fabrication of colloidal polymer nanocomposites, *Adv. Colloid Interface Sci.*, 2009, **147–148**, 319–332, DOI: 10.1016/j.cis.2008.06.002.

3 S. Schmidt, P. A. L. Fernandes, B. G. De Geest, M. Delcea, A. G. Skirtach, H. Möhwald and A. Fery, Release properties of pressurized microgel templated capsules, *Adv. Funct. Mater.*, 2011, **21**, 1411–1418, DOI: 10.1002/adfm.201002200.

4 A. P. Griset, J. Walpole, R. Liu, A. Gaffey, Y. L. Colson and M. W. Grinstaff, Expansile nanoparticles: synthesis, characterization, and *in vivo* efficacy of an acid-responsive polymeric drug delivery system, *J. Am. Chem. Soc.*, 2009, **131**, 2469–2471, DOI: 10.1021/ja807416t.

5 V. Vergaro, F. Scarlino, C. Bellomo, R. Rinaldi, D. Vergara, M. Maffia, F. Baldassarre, G. Giannelli, X. C. Zhang, Y. M. Lvov and S. Leporatt, Drug-loaded polyelectrolyte microcapsules for sustained targeting of cancer cells, *Adv. Drug Delivery Rev.*, 2011, **63**, 847–864, DOI: 10.1016/j.addr.2011.05.007.

6 D. Mishra, H. C. Kang and Y. H. Bae, Reconstitutable charged polymeric $(PLGA)_2$-*b*-PEI micelles for gene therapeutics delivery, *Biomaterials*, 2011, **32**, 3845–3854, DOI: 10.1016/j.biomaterials.2011.01.077.

7 D. Brambilla, B. L. Droumaguet, J. Nicolas, S. H. Hashemi, L. P. Wu, S. M. Moghimi, P. Couvreur and K. Andrieux, Nanotechnologies for Alzheimer's disease: diagnosis, therapy, and safety issues, *Nanomed.: Nanotechnol., Biol. Med.*, 2011, **7**, 521–540, DOI: 10.1016/j.nano.2011.03.008.

8 S. S. Rajan, H. Y. Liu and T. Q. Vu, Ligand-bound quantum dot probes for studying the molecular scale dynamics of receptor endocytic trafficking in live cells, *ACS Nano*, 2008, **2**, 1153–1166, DOI: 10.1021/nn700399e.

9 J. Yan, M. C. Est_evez, J. E. Smith, K. Wang, X. He, L. Wang and W. Tan, Dye-doped nanoparticles for bioanalysis, *Nano Today*, 2007, **2**, 44–50, DOI: 10.1016/S1748-0132(07)70086-5.

10 C. Tekle, B. Deurs, K. Sandvig and T. G. Iversen, Cellular trafficking of quantum dot-ligand bioconjugates and their induction of changes in normal routing of unconjugated ligands, *Nano Lett.*, 2008, **8**, 1858–1865, DOI: 10.1021/nl0803848.

11 W. I. Hagens, A. G. Oomen, W. H. de Jong, F. R. Cassee and A. J. A. M. Sips, What do we (need to) know about the kinetic properties of nanoparticles in the body?, *Regul. Toxicol. Pharmacol.*, 2007, **49**, 217–229, DOI: 10.1016/j.yrtph.2007.07.006.

12 J. Dobson, Toxicological aspects and applications of nanoparticles in paediatric respiratory disease, *Paediatr. Respir. Rev.*, 2007, **8**, 62–66, DOI: 10.1016/j.prrv.2007.02.005.

13 Y. Y. Zhang, L. Hu and C. Y. Gao, Influence of silica particle internalization on adhesion and migration of human dermal fibroblasts, *Biomaterials*, 2010, **31**(32), 8465–8474, DOI: 10.1016/j.biomaterials.2010.07.060.

14 Arnida, A. Malugin and H. Ghandehari, Cellular uptake and toxicity of gold nanoparticles in prostate cancer cells: a comparative study of rods and spheres, *J. Appl. Toxicol.*, 2010, **30**, 212–217, DOI: 10.1002/jat.1486.

15 S. M. Moghimi, A. J. Andersen, D. Ahmadvand, P. P. Wibroe, T. L. Andresen and A. C. Hunter, Material properties in complement activation, *Adv. Drug Delivery Rev.*, 2011, **63**, 1000–1007, DOI: 10.1016/j.addr.2011.06.002.

16 P. O. Andersson, C. Lejon, B. Ekstrand-Hammarström, C. Akfur, L. Ahlinder, A. Bucht and L. Österlund, Polymorph- and size-dependent uptake and toxicity of TiO2 nanoparticles in living lung epithelial cells, *Small*, 2011, **7**, 514–523, DOI: 10.1002/smll.201001832.

17 M. R. Lorenz, V. Holzapfel, A. Musyanovych, K. Nothelfer, P. Walther, H. Frank, K. Landfester, H. Schrezenmeier and V. Mailänder, Uptake of functionalized, fluorescent-labeled polymeric particles in different cell lines and stem cells, *Biomaterials*, 2006, **27**, 2820–2828, DOI: 10.1016/j.biomaterials.2005.12.022.

18 B. D. Chithrani and W. C. W. Chan, Elucidating the mechanism of cellular uptake and removal of protein-coated gold nanoparticles of different sizes and shapes, *Nano Lett.*, 2007, **7**(6), 1542–1550, DOI: 10.1021/nl070363y.

19 Y. Geng, P. Dalhaimer, S. Cai, R. Tsai, M. Tewari, T. Minko and D. Discher, Shape effects of filaments *versus* spherical particles in flow and drug delivery, *Nat. Nanotechnol.*, 2007, **2**(4), 249–255, DOI: 10.1038/nnano.2007.70.

20 V. Vergaro, E. Abdullayev, Y. M. Lvov, A. Zeitoun, R. Cingolani, R. Rinaldi and S. Leporatti, Cytocompatibility and uptake of halloysite clay nanotubes, *Biomacromolecules*, 2010, **11**(3), 820–826, DOI: 10.1021/bm9014446.

21 M. R. Jones, K. D. Osberg, R. J. Macfarlane, M. R. Langille and C. A. Mirkin, Templated techniques for the synthesis and assembly of plasmonic nanostructures, *Chem. Rev.*, 2011, **111**(6), 3736–3827, DOI: 10.1021/cr1004452.

22 T. J. Lei, S. Srinivasan, Y. Tang, R. Manchanda, A. Nagesetti, A. Fernandez-Fernandez and A. J. McGoron, Comparing cellular uptake and cytotoxicity of targeted drug carriers in cancer cell lines with different drug resistance mechanisms, *Nanomed.: Nanotechnol., Biol. Med.*, 2011, **7**, 324–332, DOI: 10.1016/j.nano.2010.11.004.

23 A. G. Tkachenko, H. Xie, D. Coleman, W. Glomm, J. Ryan, M. F. Anderson, S. Franzen and D. L. Feldheim, Multifunctional gold nanoparticle–peptide complexes for nuclear targeting, *J. Am. Chem. Soc.*, 2003, **125**(16), 4700–4701, DOI: 10.1021/ja0296935.

24 F. Rehfeldt, A. J. Engler, A. Eckhardt, F. Ahmed and D. E. Discher, Cell responses to the mechanochemical microenvironment-implications for regenerative medicine and drug delivery, *Adv. Drug Delivery Rev.*, 2007, **59**, 1329–1339.

25 A. Engler, L. Richert, J. Y. Wong, C. Picart and D. E. Discher, Surface probe measurements of the elasticity of sectioned tissue, thin gels and polyelectrolyte multilayer films: correlations between substrate and cell adhesion, *Surf. Sci.*, 2004, **570**, 142–154.

26 K. A. Beningo and Y. L. Wang, Fc-receptor-mediated phagocytosis is regulated by mechanical properties of the target, *J. Cell Sci.*, 2002, **115**, 849–856.

27 X. Banquy, F. Suarez, A. Argaw, J. M. Rabanel, P. Grutter, J. F. Bouchard, P. Hildgen and S. Giasson, Effect of mechanical properties of hydrogel nanoparticles on macrophage cell uptake, *Soft Matter*, 2009, **5**, 3984–3991, DOI: 10.1039/b821583a.

28 L. Hu, Z. W. Mao and C. Y. Gao, Colloidal particles for cellular uptake and delivery, *J. Mater. Chem.*, 2009, **19**, 3108–3115, DOI: 10.1039/b815958k.

29 D. P. Aden, A. Vogel, S. Plotkin, I. Damjanov and B. B. Knowles, Controlled synthesis of HBS Ag in a differentiatedhuman liver carcinoma-derived cell line, *Nature*, 1979, **282**, 615–616.

30 B. Neises and W. Steglich, Simple method for the esterification of carboxylic acids, *Angew. Chem., Int. Ed. Engl.*, 1978, **17**, 522–524, DOI: 10.1002/anie.197805221.

31 D. Walczyk, F. B. Bombelli, M. P. Monopoli, I. Lynch and K. A. Dawson, What the cell "Sees" in bionanoscience, *J. Am. Chem. Soc.*, 2010, **132**(16), 5761–5768, DOI: 10.1021/ja910675v.

32 L. Vroman, *et al.*, Interaction of high molecular-weight kininogen, factor-XII, and fibrinogen in plasma at interfaces, *Blood*, 1980, **55**(1), 156–159.

33 B. D. Chithrani and W. C. W. Chan, Elucidating the mechanism of cellular uptake and removal of protein-coated gold nanoparticles of different sizes and shapes, *Nano Lett.*, 2007, **7**(6), 1542–1550, DOI: 10.1021/nl070363y.

34 K. Y. Win and S. S. Feng, Effects of particle size and surface coating on cellular uptake of polymeric nanoparticles for oral delivery of anticancer drugs, *Biomaterials*, 2005, **26**(15), 2713–2722.

35 Y. Y. Zhang, L. Hu, D. H. Yu and C. Y. Gao, Influence of silica particle internalization on adhesion and migration of human dermal fibroblasts, *Biomaterials*, 2010, **31**(32), 8465–8474, DOI: 10.1016/j.biomaterials.2010.07.060.

36 M. D. Chavanpatil, A. Khdair and J. Panyam, Nanoparticles for cellular drug delivery: mechanisms and factors influencing delivery, *J. Nanosci. Nanotechnol.*, 2006, **6**(9–10), 2651–2663, DOI: 10.1166/jnn.2006.443.

37 G. Sahay, D. Y. Alakhova and A. V. Kabanov, Endocytosis of nanomedicines, *J. Controlled Release*, 2010, **145**(3), 182–195, DOI: 10.1016/j.jconrel.2010.01.036.

38 H. Y. Nam, S. M. Kwon, H. Chung, S. Y. Lee, S. H. Kwon, H. Jeon, Y. Kim, J. H. Park, J. Kim, S. Her, Y. K. Oh, I. C. Kwon, K. Kim and S. Y. Jeong, Cellular uptake mechanism and intracellular fate of hydrophobically modified glycol chitosan nanoparticles, *J.*


 

*Controlled Release*, 2009, **135**(3), 259–267, DOI: 10.1016/j.jconrel.2009.01.018.
39 C. Lamaze and S. L. Schmid, The emergence of clathrin-independent pinocytic pathways, *Curr. Opin. Cell Biol.*, 1995, **7**, 573–580, DOI: 10.1016/0955-0674(95)80015-8.
40 L. H. Wang, K. G. Rothberg and R. G. W. Anderson, Mis-assembly of clathrin lattices on endosomes reveals a regulatory switch for coated pit formation, *J. Cell Biol.*, 1993, **123**, 1107–1117, DOI: 10.1083/jcb.123.5.1107.
41 L. J. Hewlett, A. R. Prescott and C. Watts, The coated pit and macropinocytic pathways serve distinct endosome populations, *J. Cell Biol.*, 1994, **124**, 689–703, DOI: 10.1083/jcb.124.5.689.
42 A. Baun, N. B. Hartmann, K. Grieger and K. O. Kusk, Ecotoxicity of engineered nanoparticles to aquatic invertebrates: a brief review and recommendations for future toxicity testing, *Ecotoxicology*, 2008, **17**(5), 387–395, DOI: 10.1007/s10646-008-0208-y.
43 A. E. Nel, L. Mädler, D. Velegol, T. Xia, E. M. V. Hoek, P. Somasundaran, F. Klaessig, V. Castranova and M. Thompson, Understanding biophysicochemical interactions at the nano–bio interface, *Nat. Mater.*, 2009, **8**(7), 543–557, DOI: 10.1038/nmat2442.
44 W. H. De Jong and P. J. A. Borm, Drug delivery and nanoparticles: applications and hazards, *Int. J. Nanomed.*, 2008, **3**(2), 133–149, DOI: 10.2147/IJN.S596.
45 R. J. Pelham and Y. L. Wang, Cell locomotion and focal adhesions are regulated by substrate flexibility, *Proc. Natl. Acad. Sci. U. S. A.*, 1997, **94**, 13661–13665.
46 D. E. Discher, D. J. Mooney and P. W. Zandstra, Growth factors, matrices, and forces combine and control stem cells, *Science*, 2009, **324**, 1673–1677.